Absolute Calibration of a Geodetic Time Transfer System

John Plumb, Kristine M. Larson, Joe White, and Ed Powers

***Abstract*— An absolute calibration technique is developed for geodetic GPS receivers. An uncertainty budget for the system (receiver, cables, connectors, antenna) is evaluated, yielding 1.1 ns at each frequency, and 1.6 ns for a two-receiver experiment. Analysis of data on a short baseline yields 0.8 and 1.2 ns agreement on $P1$ and $P2$, respectively.**

***Index Terms*— IEEEtran, journal, LATEX, paper, template.**

I. Introduction

GPS receivers used in the geodetic community typically track both $L1$ (1575.42 MHz) and $L2$ (1227.60 MHz) frequencies and report both carrier phase and P-code pseudorange observables. Positions of the GPS receivers are subsequently estimated using least squares analysis of the observations. If the clocks are modeled explicitly, pseudorange data are used in addition to the carrier phase data. In geodetic analysis, the range between each satellite and antenna is modeled, meaning that precise ephemerides must be available. In addition to clocks, other significant error sources such as atmospheric delays, and carrier phase ambiguities are estimated or modeled. For many geophysical applications, positions based on 24-hour averages are sufficient and thus data collection and geodetic analysis strategies have been developed for 24-hour datasets. With the complete GPS constellation and 24-hour averages, geodesists report positioning precisions of 2-4 mm horizontally and 6-10 mm vertically [1].

Many timing receivers use the same physical device as geodetic receivers but use firmware that by convention reports $L1$ C/A-code pseudorange only. Rather than model the full observables, pseudorange data from timing receivers are generally differenced and analyzed using the common-mode technique [2]. A geodetic time transfer system (GETT) uses geodetic receivers and models and software developed for high-precision positioning to estimate clock behavior. A GETT system has been evaluated over the past 15 years, in a series of papers starting in 1990 [3]–[10]. Researchers using different GETT strategies have reported frequency stability of 2-5 parts in 10^{15} over one day [11]–[14].

In parallel with efforts to demonstrate GETT frequency stability, there has been a significant effort to calibrate geodetic receivers for time transfer applications. Differential calibration of geodetic receivers is one method for measuring relative signal path delays between two receivers [15]. To accomplish this, a receiver is circulated among timing laboratories. A relative calibration is then performed with respect to the timing laboratory receiver. Subsequent comparisons between timing laboratories use these relative calibrations.

Manuscript received X; revised Y. This research was supported by NRL contract XX and NSF grant YY.

Alternatively, an absolute calibration method has been developed for GETT [16]–[19]. In this method, individual GETT receivers are calibrated with respect to a GPS simulator. The purpose of this report is to further describe the calibration technique for GETT receivers and to develop an uncertainty budget. The GETT calibrations were subsequently tested in controlled experiments. Systematic errors related to the calibration's accuracy are also discussed. In a companion paper, calibrated GETT systems are compared against calibrated TWSTFT (Two-Way Satellite Time and Frequency Transfer) links [20].

II. GPS Receiver Calibration

We report a repeatable absolute calibration technique which can be used to measure the electrical delays for a geodetic receiver. Specifically, the delay of an Ashtech Z-12T receiver can be measured relative to a GPS signal simulator [19]. By also measuring delays for an antenna and the cables, an overall delay (and accompanying uncertainty budget) for a geodetic timing system can be calculated.

The Ashtech Z-12T receiver was chosen for this study because it has a repeatable internal reference. This internal reference is determined by the difference in the time of arrival at the receiver of the input 20 MHz signal and the input one pulse per second (1 PPS) signal. Because the 20 MHz and 1 PPS inputs to the receiver must be coherent and externally generated, the calibration delay remains the same when the receiver power is cycled. This is in direct contrast to other geodetic receivers, in which the overall receiver delay "resets" with each power cycle [21].

A. Equipment Setup

The experimental set-up is shown in Figure 1. The GPS signal simulator (Global Simulation Systems model 2760 GPS) produces a 1 PPS output. The pulse is sharpened by the USNO 1 PPS amplifier, allowing more accurate measurements. The simulator 1 PPS is input to the geodetic GPS receivers and a fixed relationship between the simulated pseudorange code transition and the 1 PPS entering each receiver can be established. It is this fixed relationship that allows the calculation of the receiver delay. The simulator RF, the 20 MHz, and the 1 PPS signals are split and sent to the receivers being calibrated.

B. Measuring the Tick-to-Code Delay

A GPS signal simulator generates code pseudorange signals on both the $L1$ and $L2$ frequencies (hereafter termed $P1$ and

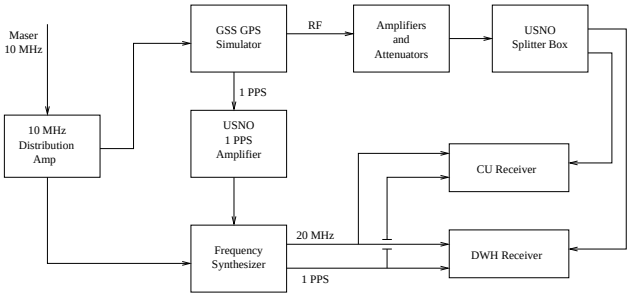

Fig. 1. Equipment setup for calibration of receivers CU and DWH. Attenuating RF pads and DC blocks at the receiver RF input are not shown.

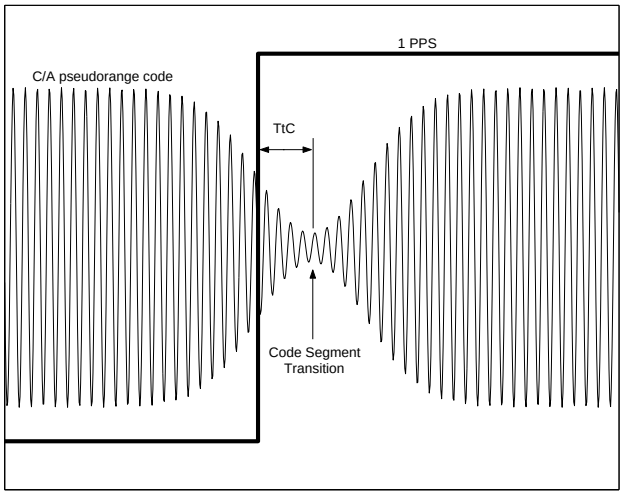

Fig. 2. Measuring the Tick-to-Code delay. The figure shows a positive TtC.

$P2$ for the P-code observables). By simulating a satellite range of zero, and amplifying the simulated signal enough to make it visible on a fast digital oscilloscope, the difference in the time of arrival between the rising 1 PPS and the pseudorange code transition can be measured. The rising 1 PPS signal is measured at the point it achieves one volt. The delay between these two points is referred to as the Tick-to-Code (TtC) delay (Figure 2). Inherent to the simulator and the electrical path of Figure 1, the TtC delay represents the difference between the satellite clock and the receiver clock. This is possible because the GPS simulator generates a 1 PPS output coherent with the simulated RF signal, which means that the pulses are fixed with respect to the simulated pseudorange. Because the electrical delays in Figure 1 remain constant, the TtC delay remains constant. Final TtC values must also account for the delays of connectors, DC blocks, and attenuating pads in the experimental setup. The oscilloscope screen for the P-code is shown in Figure 3.

In order to determine a calibration delay for the receiver, the measured TtC delay will be subtracted from the pseudoranges recorded by the receiver. In a typical set-up, the input 1 PPS would be generated by the timing laboratory's clock, and the TtC value would vary with time as the satellite and laboratory clocks vary. In all cases, the TtC delays are measured at the inputs to the receiver. In order to perform the TtC measurement, the simulated RF signal must be significantly amplified

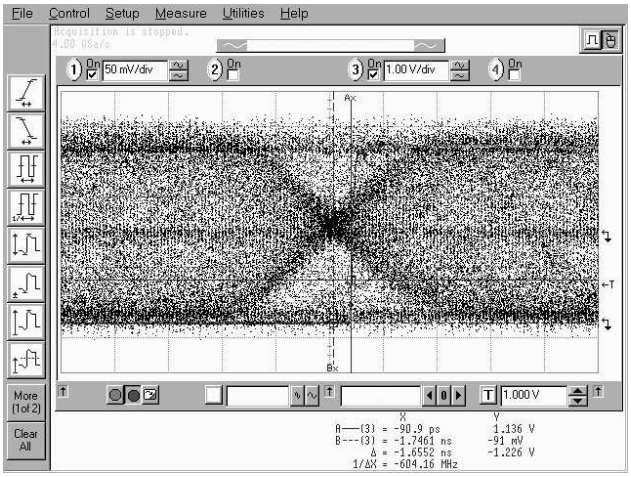

Fig. 3. Oscilloscope screen during TtC measurement for $P1$ (TtC delay = -1.66 ns).

in order to observe the code transition on an oscilloscope. The amplified signal cannot be injected directly into the receiver. Instead, it must first be passed through RF attenuating pads. During the calibrations, 60-80 dB of attenuation were required between the RF signal cable and the back of the receiver. The attenuating pads used produce a delay in the simulated GPS signal that must be accounted for when computing the true TtC delay. For example, if the attenuating pads delay the GPS signal by 0.4 ns, that amount must be added to the TtC value measured on the oscilloscope. Furthermore, each receiver provides DC power for the antenna pre-amplifier through the antenna cable. This DC power signal must be blocked to prevent the voltage from interfering with other equipment in the experiment. The delay of the GPS signal through the DC block must also be accounted for when calculating the true TtC delay.

A vector network analyzer was used to measure the delays through the RF attenuating pad and DC block. Unfortunately the entire chain of pads and DC block cannot be measured simultaneously because the attenuation is too great. Instead, each component must be measured individually, and the results combined. The receivers that were calibrated require N-type connectors for the RF input, but the oscilloscope used required a BNC connector. In order to be rigorous, any differences in the delays of these two connectors must also be taken into account. The uncertainty in each measurement (DC block, attenuating pads, connectors) was taken to be 0.1 ns at each frequency, based on the repeatability of the measurements. Measurement uncertainty of the TtC delay using the oscilloscope is taken to be 0.2 ns, again based on the repeatability of the measurement. While each of these components individually constitutes a delay that is a fraction of a ns, their combined uncertainty increases the overall calibration uncertainty budget.

C. Measuring the Tick-to-Phase Delay

As previously mentioned, Ashtech Z-12T receivers can be calibrated because the internal reference is repeatable. The 20 MHz zero crossing that immediately follows the rising tick of

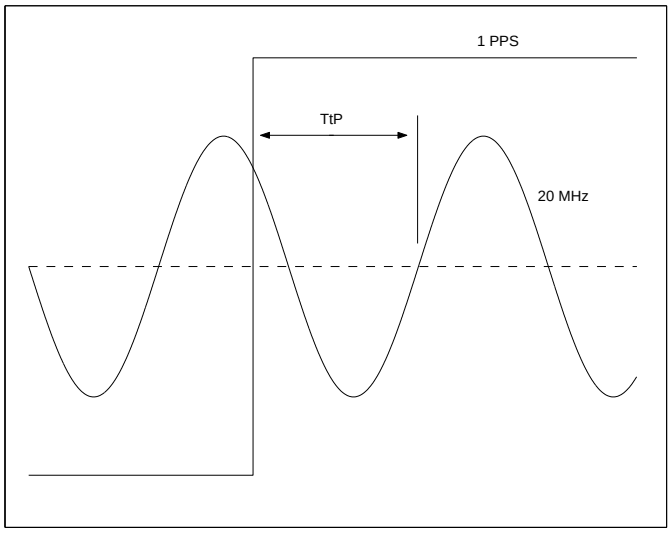

Fig. 4. Measuring the Tick-to-Phase Delay (TtP).

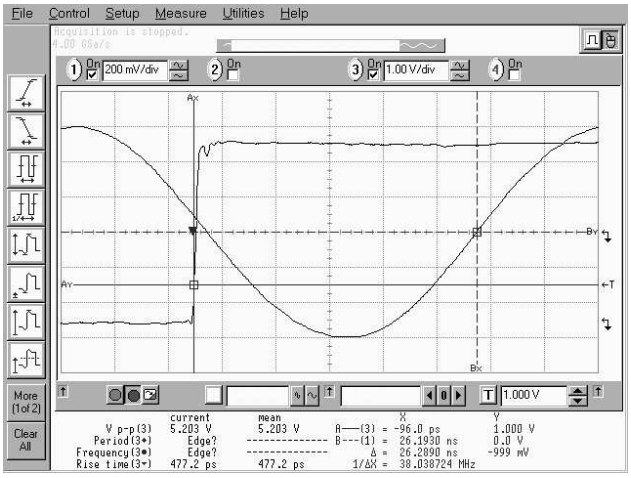

Fig. 5. Oscilloscope screen during TtP measurement (TtP delay = 26.29 ns).

the 1 PPS signal marks the internal reference (zero) time for the receiver. Whether this internal reference is marked by the rising or falling 20 MHz zero can be determined by opening the receiver case and inspecting the jumper on the circuit board: its position is clearly marked as rising or falling. All of the receivers used in this experiment were configured for the rising zero. The time difference between the 1 PPS rising tick and the next rising zero of the 20 MHz clock is called the Tick-to-Phase (TtP) delay. The TtP is explained graphically in Figure 4. An oscilloscope screen captured during the TtP measurement is shown in Figure 5.

When measuring the TtP or TtC delays, the 1 PPS input does not have a zero rise time. Therefore, in all cases the rising 1 PPS signal is measured at the point it achieves 1 volt. As with the TtC measurement, the accuracy of determining the TtP is taken to be 0.2 ns. The measurement is taken as the signals enter the receiver.

Receiver	TtP Interval	P1 ns	P2 ns	P3 ns
CU	12.0 - 58.9	294.8-TtP	308.0-TtP	274.4-TtP
DWH	9.0 - 50.0	290.2-TtP	304.4-TtP	268.3-TtP

TABLE I
RECEIVER DELAY CALIBRATION RESULTS.

D. Calculating the Receiver Delay

Once the TtC delay is known, a linear calibration curve can be derived. The receiver's reported range (RR) will be too large by the combination of the receiver delay and the TtC delay. Using the simulated true range (TR) to the receiver (recorded by the simulator) and the measured TtC, the receiver delay, as a function of TtP, is calculated as follows:

$$RR - TR - TtC = ReceiverDelay(TtP) \quad (1)$$

The frequency synthesizer in Figure 1 converts the input 10 MHz clock into the 20 MHz clock output required by the Ashtech Z12-T. By triggering this output with the 1 PPS signal, the synthesizer can be used to shift the relative phase of the 20 MHz clock and 1 PPS input signals. The Tick-to-Phase was originally shifted in increments of 10 ns, for a total of 5 separate measurements spanning 40 ns. Subsequent testing allowed delay computations over a TtP interval of 46.9 ns for the CU receiver, and 41 ns for the DWH receiver. The receivers collected data at 30 second intervals during each TtP increment for approximately 20 minutes.

The receiver delay was calculated for each satellite at each observation epoch during the 20 minute measurement period. These data were used to determine an average delay. Outliers greater than three times the standard deviation were removed. This process was iterated until no outliers remained.

Fifty ns corresponds to one full cycle of the 20 MHz clock signal. Examining Table I, the TtP interval for the CU receiver extends to values greater than 50 ns. The TtP delay is determined by measuring the relationship of the two signals as they enter the receiver; the internal electrical path of the receiver is not taken into account. From entering the receiver until the signals reach the component marking the internal reference, the electrical path of the 1 PPS signal is at least 8.9 ns longer than the path for the 20 MHz signal. Any rising zero entering the receiver less than 8.9 ns after the rising 1 PPS will arrive at the marking component before the 1 PPS signal does. The next rising zero, which occurs 50 ns later, will be the first rising zero to arrive at the marking component after the tick. For example, if the measured TtP delay is 5 ns, the rising zero at 55 ns will mark the internal timing reference.

The exact amount each receiver delays its 1 PPS signal relative to its 20 MHz clock is unknown, but the value is bounded by the gap produced by the data collection method. The TtP value that causes this crossover could be determined by using smaller increments when data are collected.

Although geodetic GPS receivers record observations at $L1$ and $L2$, time transfer experiments require that the ionosphere-free ($P3$) linear combination be used. The equivalent $P3$

receiver delay δP3 is calculated as follows:

$$\delta P3 = \frac{f_1^2}{f_1^2 - f_2^2} * \delta P1 - \frac{f_2^2}{f_1^2 - f_2^2} * \delta P2 \quad (2)$$

$$\delta P3 \approx 2.545 * \delta P1 - 1.545 * \delta P2 \quad (3)$$

III. Receiver Calibration Uncertainty Budget

In order to determine the total delay of a GPS receiver, several different measurements must be evaluated. The simulator's output truth ranges are known to be precise, but their accuracy is unknown. A conservative estimate places the simulator accuracy at 1 ns [19]. This value is based on an external measurement where the phase from channel 1 is compared to the 1 pulse per second tick that the simulator provides. This is done manually using a high-speed digital oscilloscope. We compare position of the dip in the signal envelope to the 1 PPS signal. The resolution of this method is $\sim$ 0.5 ns. Repeated measurements of this property over time have shown that it is stable to better than 1 ns. Accumulating all of the measurement errors results in the uncertainty budget detailed in Table II. Whenever possible, uncertainty estimates were determined by computing a standard deviation. Assuming a single-frequency uncertainty of 1.1 ns and that the uncertainties on the two frequencies are independent yields an uncertainty of 3.2 ns when using the ionosphere-free observable combination (Table IV). This is a conservative uncertainty estimate as it is unlikely that the single-frequency uncertainties are independent, especially for the simulator.

Uncertainty Source	Estimate(ns)
Tick-to-Phase	0.2
Tick-to-Code	0.2
Delay in RF pads	0.1
Delay in connectors	0.1
Delay in DC block	0.1
Simulator Accuracy	1.0
Frequency Synthesizer	0.2
$\sqrt{\Sigma\epsilon_i^2}$	1.1

TABLE II
SINGLE-FREQUENCY MEASUREMENT UNCERTAINTIES FOR GPS RECEIVER CALIBRATION.

IV. Antenna calibration

Calibrations of the GPS antenna and the antenna cable are also needed to develop an accurate time transfer uncertainty budget. The antenna cable's electrical length can be measured with a vector network analyzer for each GPS frequency to an accuracy of $\sim$ 0.1 ns. Calibration of a GPS antenna is more complicated. In order to determine the delay through the antenna for both GPS frequencies, an anechoic chamber was used in concert with a vector network analyzer and a separate radiating antenna (Figure 6). The delay is measured in three separate steps.

First, a flat metal sheet is placed in the anechoic chamber where the antenna will eventually rest. The goal is to measure

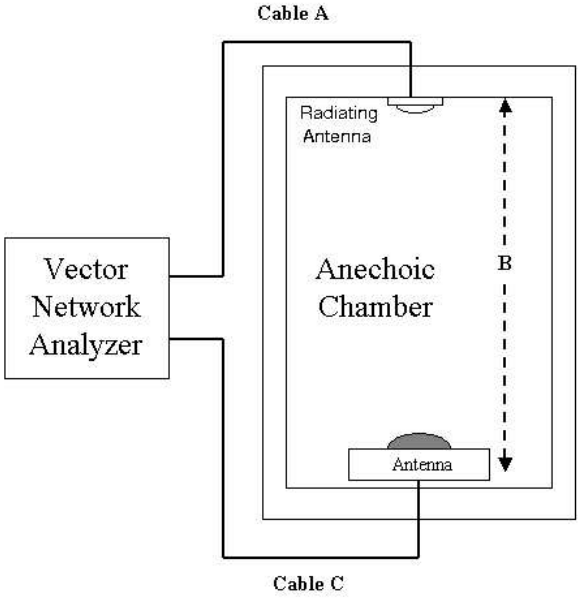

Fig. 6. Antenna calibration setup. Chamber height is approximately 3 m.

the electrical length of cable A, plus the radiating antenna (ANT_{rad}) and the air in the chamber (length B). The electrical length is determined by measuring the reflected peak caused by the flat metal surface. In the second step, the electrical length of cable C from the antenna back to the vector network analyzer is measured. Finally, cable C is attached to the antenna and is placed inside the chamber. Power is supplied to the antenna with an inline bias-tee (not shown), since the antenna pre-amplifier needs to be powered in order to properly measure its delay. The vector network analyzer is then used to measure the total delay through: cable A, the radiating antenna, the air in the chamber, the antenna being calibrated, and cable C. The antenna delay ANT_δ is then measured as follows:

$$ANT_\delta = TOT_\delta - (A + ANT_{rad} + B) - C \quad (4)$$

The uncertainties in this measurement are summarized in Table III. There is some concern that calibrating the antenna by measuring the delay for the central GPS frequency does not properly account for the delay of the pseudorange, which has a bandwidth of close to 20 MHz. Phase center variations are also not accounted for in this calibration. Because phase center variations are on the order of 2 cm, their effect is expected to be less than 0.1 ns, which is less than the uncertainty budget for the calculation. The impact of phase center variations on time transfer accuracy can be mitigated by using calibration values [22]. As with the receiver calibration, the single-frequency antenna uncertainty of 0.2 ns yields an uncertainty of 0.6 ns when using the ionosphere-free observable combination. A weakness of our analysis is that only one antenna was calibrated. The precision of this calibration method should, at a minimum, be examined further by calibrating all antennas used for geodetic time transfer experiments.

Uncertainty Source	Estimate
Cable A/ Chamber	0.1
Cable C	0.1
Total Delay	0.1
$\sqrt{\Sigma\epsilon_i^2}$	0.2

TABLE III
SINGLE FREQUENCY MEASUREMENT UNCERTAINTIES FOR ANTENNA CALIBRATION. ALL VALUES IN NS.

Uncertainty Source (Simulator,ns)	P1 Estimate ns (1.0)	P3 Estimate ns (1.0)	P3 Estimate ns (0.0)
Antenna	0.2	0.6	0.6
Antenna Cable	0.1	0.3	0.3
Receiver	1.1	3.2	1.2
Tick-to-Phase	0.2	0.2	0.2
1 PPS link	0.1	0.1	0.1
$\sqrt{\Sigma\epsilon_i^2}$	1.1	3.3	1.4

TABLE IV
UNCERTAINTIES FOR GETT CALIBRATION.

V. GETT UNCERTAINTY BUDGET

The total uncertainty budget for a GPS system is summarized in Table IV. For completeness, two more measurements have been added. The accuracy of the 1 PPS (the "tick") link from the clock to the receiver is also a factor in the overall time transfer and is not frequency dependent. This value should be known to the accuracy of a cable measurement, which is taken to be 0.1 ns. A TtP measurement must be taken when setting up the receiver in order to determine the calibration value. As before, the TtP can be measured within an uncertainty of 0.2 ns. Because these values are only measured once, their impact on the ionosphere-free uncertainty budget is the same as their impact on the single-frequency uncertainty budget.

Assuming that the $P1$ and $P2$ errors are independent, the $P3$ GETT calibration uncertainty is 3.3 ns (Table IV). The dominant term in this calibration is the unknown accuracy of the simulator. If the simulator uncertainty is reduced to 0.5 or 0.0 ns, the overall calibration accuracy drops to 2.0 and 1.4 ns, respectively. For time transfer between receivers calibrated with the same simulator, it is entirely possible that the relative simulator uncertainty is much less than the 1 ns value assumed for this study.

VI. ZERO-BASELINE EXPERIMENT

Receiver and antenna calibrations can be externally validated in a "short-baseline" or "zero-baseline" experiment [15]. Over short distances, many GPS error sources (orbits, atmospheric refraction) are insignificant. For the zero-baseline case, one antenna is connected to each receiver. This test is insensitive to the antenna delay and multipath; a short-baseline test is sensitive to both. We had access to two calibrated receivers for a several week period, but as stated previously, only one calibrated antenna. We are thus only able to evaluate the relative $P1$ and $P2$ receiver calibration values.

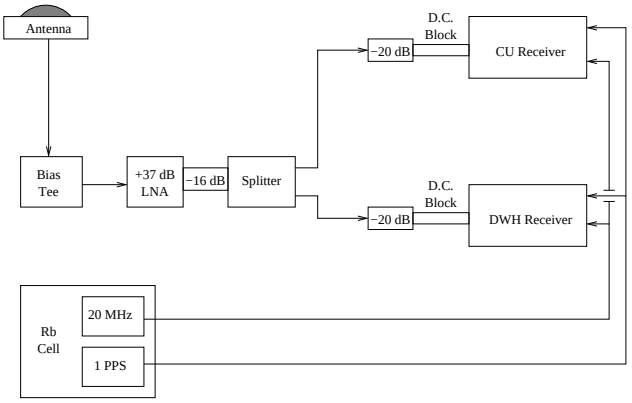

Fig. 7. Zero baseline experimental setup.

In a companion paper [20], comparisons of calibrated GETT receiver/antenna systems with calibrated TWSTFT systems on longer baselines are discussed.

The hardware setup for the zero-baseline experiment is summarized in Figure 7. A rubidium cell provided both a 10 MHz and 1 PPS output to each GPS receiver. The 10 MHz output was converted to a 20 MHz signal using a function generator. A single antenna feeds a low noise amplifier (LNA) followed by a splitter. The split signal is sent to each receiver via a short cable and RF attenuating pads. A D.C. block is used on each antenna as well; antenna power is supplied via a bias tee upstream of the splitter. The amplifier and pads are essential to prevent coherent interference from signal reflections off of the splitter and amplifier.

Care must be taken not to allow signal reflections from inline components to introduce cable multipath errors into the GPS observations. Cable multipath occurs due to impedance mismatches between the antenna cable and the receiver (or other components). If the impedance mismatch between the antenna cable and the receiver is high enough, a part of the injected signal is reflected off the receiver back toward the antenna. This reflected signal can also be reflected off of the antenna cable/antenna interface, then back into the receiver. If the round trip time is short enough to allow this reflected signal to interfere with the receiver's delay lock loop correlator, a constant contribution due to cable multipath can be expected in the clock estimates [23]. To mitigate the impedance mismatch at the antenna cable/receiver interface, 20 dB of attenuation was inserted at that boundary. Any cable multipath reflections injected into the receiver would have to pass through this attenuator two more times than the original signal, virtually eliminating the reflected signal. This caused another problem, however: the receiver could not operate effectively with the incoming antenna signal reduced by 20 dB. To combat this loss, a Low Noise Amplifier (LNA) was inserted into the antenna cable signal path. In this experiment, the LNA had a gain of +37 dB. The signal was attenuated by 16 dB immediately upon exiting the LNA. Thus the 37 dB in gain is offset by 36 dB of loss due to attenuating pads. Achieving a proper balance between amplification and attenuation directly contributed to the success of this experiment.

In a zero-baseline experiment, any component upstream

of the splitter provides a common delay to both receivers. Therefore, the only delays that need to be accounted for are the splitter, the path from the splitter to the receiver, and the receiver itself. The splitter, cables, RF pads, and DC blocks were chosen to be closely matched. A conservative estimate for the difference in the path lengths is 0.3 ns. Utilizing Table I, the Tick-to-Phase values were 12.2 ns for DWH and 14.5 ns for CU. This results in differential calibration values of 2.3 and 1.3 ns for $P1$ and $P2$, respectively. By differencing and averaging the measured $P1$ and $P2$ values (using an elevation angle cutoff of 15 degrees), we estimated these values to be 3.07 and 2.49 ns. The standard deviations of the $P1$ and $P2$ differences were 1.01 and 1.08 ns, respectively. Thus, the differenced $P1$ and $P2$ values agree with the simulator calibrations to 0.8 and 1.2 ns, within set-up uncertainty (0.3 ns) and the single frequency uncertainty budget for a baseline of 1.6 ns ($1.1 * \sqrt{2}$). A zero-baseline experiment is ideal for validating our calibration results, but is not representative of the system's accuracy for typical usage. The accuracy of GETT time transfer will degrade as multipath errors are introduced and longer baselines are used.

VII. Systematic Errors

Any time-varying influence on the GPS observables will degrade GETT time transfer accuracy. We have identified systematic errors related to power outages and temperature dependence.

A. Power Transients

Although the Ashtech Z-12T receivers are designed to return to the same calibration delay after a power cycle, we have identified a startup transient in the Z12-T receiver. This transient typically lasts 0.5-2.5 hours and clearly has an adverse effect on time transfer performance. Figure 8 shows the startup transient for the $P1$ delay after a power cycle. In this case, the transient lasted approximately 35 minutes and has a magnitude of more than 2.5 ns. The receiver calibration described in this paper assumed that the delay for a particular receiver is constant; this assumption is violated by the presence of power transients. Thus, data recorded within several hours after known power cycles should not be used for GETT estimates.

B. Thermal Errors

Temperature coefficients of GPS receiver delays have been measured to be on the order of ± 100 ps/^{o}C [9], [24]. Thus variations in receiver temperature can directly affect time transfer estimates. In order to minimize temperature errors in our long-term comparisons between GETT and TWSTFT, we isolated the CU receiver installed at NIST in a temperature chamber [20]. Although we did not set out to test the temperature dependence of the Ashtech Z-12T receiver, we observed several instances of significant temperature-related errors. As an illustration, Figure 9 shows the time transfer solution when the NIST temperature chamber (which had been turned off for approximately 48 hours) was restored to operation. The

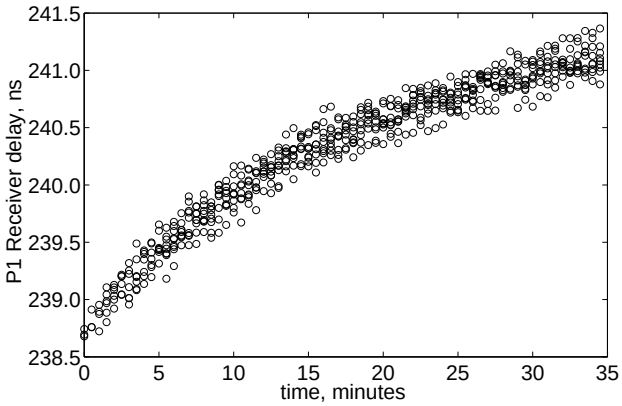

Fig. 8. Transient in $P1$ delay for an Ashtech Z-12T receiver following a power cycle.

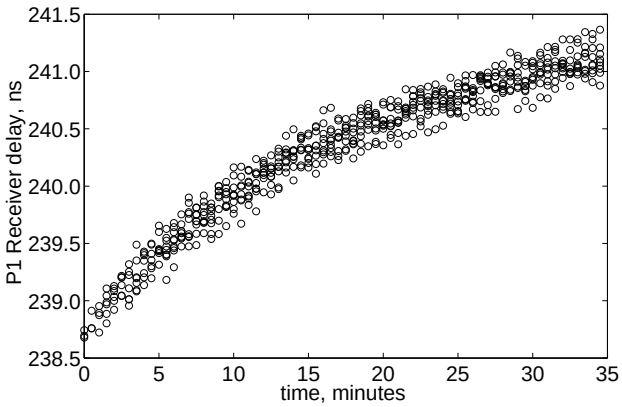

Fig. 9. Time transfer error caused by a temperature excursion at the CU receiver.

estimates exhibit a very rapid change over $\sim$30 minutes as cooling is initiated. The actual temperature change during this time is not known.

A smaller temperature effect on GETT has also been isolated. For a short period, two Ashtech Z-12T receivers were operated in the NIST temperature chamber. The temperature chamber itself was small (6 cubic feet); two receivers filled more than half the space inside. These two receivers were operated together for approximately one month. On the days the second receiver was placed in and removed from the chamber, an offset of approximately 375 ps is apparent in GETT between NIST and the Alternate Master Clock site (AMC2) in Colorado Springs. Placing the second receiver on top of the first inside the chamber altered the temperature of the first receiver enough for the effects, though small, to be observed.

In summary, to perform the best time transfer possible, the receiver must be thermally isolated from its environment. Furthermore, for calibrated delays to be accurate, the temperature inside the isolation chamber should be the same as the temperature at which the calibration was performed.

VIII. Discussion

We used the Ashtech Z-12T GPS receiver because of its repeatable internal reference. This allowed us to calibrate each

receiver with respect to a simulator, providing an absolute time transfer link. A secondary but very important result of using the Ashtech Z-12T receiver at each of our timing sites is that it allows us to minimize possible systematic errors associated with mixing GPS receivers manufactured by different companies. This is particularly true if the receivers are tracking different codes, i.e. a receiver reporting C/A could have a bias with respect to P-code pseudorange. Another source of bias is from using uncalibrated antennas. For a short baseline experiment using common antenna types, phase center variations will cancel. Using identical antenna models at all sites is generally not feasible, so it is important to use phase center calibration values [22].

IX. Conclusions

An absolute calibration system for geodetic time transfer has been developed. Each geodetic receiver to be used in the timing link is first calibrated with respect to a GPS simulator. An uncertainty budget was developed for each component of the time transfer system, yielding a 1.1 ns on each frequency for each system. For a baseline consisting of two timing systems, agreement should be $\sim$ 1.6 ns. The receiver component of our calibrations was validated in a zero-baseline test, yielding 0.8 and 1.2 ns agreement on $P1$ and $P2$, respectively. While these calibration results are promising, additional comparisons using calibrated antennas is needed. The influence of multipath on GETT accuracy should also be evaluted. Finally, GETT must be compared with other time transfer systems [20].

Acknowledgments

We thank Doug Hogarth for lending us his receiver and download software, and the IGS for high-quality GPS orbits. The GIPSY-OASIS software was made available to us by the Jet Propulsion Laboratory, California Institute of Technology. Judah Levine provided space for our equipment at NIST, an environmental chamber, access to the maser ensemble, and a storage site for the data. We also thank Christine Hackman, Jim Ray, and two anonymous reviewers for providing valuable feedback on this paper. Funding for this study was provided by NRL and NSF.

References

[1] J. Zumberge, M. Heflin, D. Jefferson, M. Watkins, and F. Webb, "Precise point positioning for the efficient and robust analysis of GPS data from a large network," *J. Geophy. Res.*, vol. 102, pp. 5005–5018, 1997.

[2] D. Allan and M. Weiss, "Accurate time and frequency transfer during common-view of a GPS satellite," in *Proc. 34th Freq. Control Symp.*, May 1980, pp. 334–356.

[3] T. Schildknecht, G. Beutler, W. Gurtner, and M. Rothacher, "Towards subnanosecond GPS time transfer using geodetic processing technique," in *Proceedings 4th EFTF*, 1990, pp. 335–346.

[4] P. Baeriswyl, T. Schildknecht, W. Gurtner, , and G. Beutler, "Frequency and time-transfer with geodetic GPS receivers," in *Proc. 7th Eur. Freq. Time Forum*, Besanlon, France, 1993, pp. 119–124.

[5] P. Baeriswyl, T. S. . T. Springer, and G. Beutler, "Frequency and time-transfer with geodetic GPS receivers: first results," in *Proc. 9th Eur. Freq. Time Forum*, Besanlon, France, 1995, pp. 46–51.

[6] P. Baeriswyl, T. Schildknecht, T. Springer, and G. Beutler, "Time-transfer with geodetic GPS receivers using code and phase observations," in *Proc. 10th Eur. Freq. Time Forum*, Neuchatel, Switzerland, 1996, pp. 430–435.

[7] C. Dunn, D. Jefferson, S. Lichten, J. Thomas, and Y. Vigue, "Time and positioning accuracy using codeless GPS," in *Proc. 25th Annual Precise Time and Time Interval (PTTI) Systems and Applications Meeting*, Marina Del Ray, California, 1993, pp. 169–182.

[8] R. Douglas and J. Popelar, "PTTI applications at the limits of GPS," in *Proc. 26th Annual Precise Time and Time Interval (PTTI) Systems and Applications Meeting*, Marina Del Ray, California, 1994, pp. 141–152.

[9] F. Overney, T. Schildknecht, G. Beutler, L. Prost, and U. Feller, "GPS time transfer using geodetic receivers: Middle-term stability and temperature dependence of the signal delays," in *Proc. 11th European Frequency and Time Forum*, 1997, pp. 504–508.

[10] F. Overney, L. Prost, G. Dudle, T. Schildknecht, G. Beutler, J. Davis, J. Furlong, and P. Hetzel, "GPS time transfer using geodetic receivers (GETT): results on European baselines," in *Proc. 12th European Frequency and Time Forum*, 1998, pp. 504–508.

[11] D. Jefferson, S. Lichten, and L. Young, "A test of precision GPS clock synchronization," in *Proc. 1996 IEEE Freq. Contr. Symp.*, Honolulu, HI, 1996, pp. 1206–1210.

[12] K. Larson and J. Levine, "Carrier-phase time transfer," *IEEE Trans. Ultrason., Ferroelect., Freq. Contr.*, vol. 46, pp. 484–494, July 1999.

[13] R. Dach, T. Schildknecht, T. Springer, G. Dudle, and L. Prost, "Recent results with transatlantic GeTT campaign," in *Proc. 31st Annual Precise Time and Time Interval (PTTI) Systems and Applications Meeting*, Dana Point, California, Dec. 1999, pp. 461–468.

[14] G. Petit, C. Thomas, Z. Jiang, P. Uhrich, and F. Taris, "Use of GPS Ashtech Z-12T receivers for accurate time and frequency comparison," *IEEE Trans*, vol. 4, pp. 941–949, 1999.

[15] G. Petit, Z. Jiang, P. Uhrich, and F. Taris., "Differential calibration of Ashtech Z12-T receivers for accurate time comparisons," in *Proceedings 14th EFTF*, 2000, pp. 40–43.

[16] G. Petit, Z. Jiang, J. White, E. Powers, G. Dudle, and P. Uhrich., "Progresses in the calibrations of geodetic like GPS receivers for accurate time comparisons," in *Proceedings 15th EFTF*, 2001, pp. 164–166.

[17] G. Petit, Z. Jiang, J. White, R. Beard, and E. Powers, "Absolute calibration of an Ashtech Z12-T GPS receiver," *GPS Solutions*, vol. 4, pp. 41–46, 2001.

[18] J. Plumb, J. White, E. Powers, K. Larson, and R. Beard, "Simultaneous absolute calibration of three geodetic timing receivers," in *Proc. 33rd Annual Precise Time and Time Interval (PTTI) Systems and Applications Meeting*, Long Beach, California, 2001.

[19] J. White, R. Beard, G. Landis, G. Petit, and E. Powers, "Dual frequency absolute calibration of a geodetic GPS receiver for time transfer," in *Proceedings of the 15th European Frequency and Time Forum (EFTF)*, 2001, pp. 167–172.

[20] J. Plumb and K. Larson, "Long-term comparisons between two way satellite and geodetic time transfer systems," *IEEE Trans. Ultrason., Ferroelect., Freq. Contr.*, 2005, in review.

[21] K. Larson, J. Levine, L. Nelson, and T. Parker, "Assessment of GPS carrier-phase stability for time-transfer applications," *IEEE Trans. Ultrason., Ferroelect., Freq. Contr.*, vol. 47, pp. 484–494, 2000.

[22] G. Mader, "GPS antenna calibration at the National Geodetic Survey," *GPS Solutions*, vol. 3, no. 1, pp. 50–58, 1999.

[23] M. Weiss, F. Ascarrunz, T. Parker, V. Zhang, and X. Gao, "Effects of antenna cables on GPS timing receivers," in *Proceeding of the 1999 Joint Meeting EFTF-IEEE IFCS*, 1999, pp. 259–262.

[24] C. Bruyninx, P. Defraigne, and J.-M. Sleewaegen, "Time and frequency transfer using GPS codes and carrier phases: Onsite experiments," *GPS Solutions*, vol. 3, no. 2, pp. 1–10, 1999.